ELSEVIER

Palaeogeography, Palaeoclimatology, Palaeoecology 181 (2002) 171–193

PALAEO

www.elsevier.com/locate/palaeo

Microfacies, sequence stratigraphy and clay mineralogy of a condensed deep-water section around the Frasnian/Famennian boundary (Steinbruch Schmidt, Germany)

X. Devleeschouwer[a,*], A. Herbosch[b], A. Préat[b]

[a] *Geological Survey of Belgium, Rue Jenner 13, B-1000 Brussels, Belgium*

[b] *Department of Earth and Environmental Sciences, University of Brussels, P.O. Box 160/02, Av. F.D. Roosevelt 50, B-1050 Brussels, Belgium*

Accepted 6 December 2001

Abstract

A multidisciplinary analysis (microfacies, sequential stratigraphy and clay mineralogy) was made on Frasnian/Famennian (F/F) boundary strata of the Steinbruch Schmidt section in Western Germany. Three major microfacies are recognised. Their succession records a shallowing-upward evolution from deep, quiet and poorly oxygenated environments, below the storm wave base, to environments influenced by current activities close to the storm wave base. The Kellwasser Horizons correspond to the deepest microfacies. The shallowest microfacies correspond to fine-grained calcareous tempestites or turbidites coming from a distant shelf of northwest Germany. The sequential pattern through the F/F boundary shows the succession of seven systems tracts. Two sequence boundaries are located just above the Lower Kellwasser Horizon and at the F/F boundary itself. These are underlined by hardgrounds suggesting time gaps. The Kellwasser Horizons correspond to sea-level highstands and the overlying beds record a transition from lowstand to transgressive systems tracts. Illite and kaolinite are the dominant clay minerals associated with mixed layers and traces of chlorite. Illite abundance is maximal during Kellwasser Horizons. Illite and kaolinite were probably inherited from a highly weathered source area although part of the illite is diagenetic. Kaolinite is the second most abundant clay mineral and is particularly well represented (up to 50%) between the Kellwasser Horizons. An unusual clay assemblage of illite and mixed layers is associated with a bentonite layer. Kaolinite increases during times when thin tempestites or turbiditic microbioclastic layers come from a distant shelf during sea-level falls. The kaolinite percentage reaches its maximum at the top of the lowstand systems tract. The high percentage of kaolinite suggests a hot–wet climate and could be related to global warming.

Keywords: microfacies; sequential analysis; clay mineralogy; Frasnian/Famennian boundary; Kellwasser Event; Germany

1. Introduction

The Frasnian/Famennian (F/F) boundary is related on a global scale to the presence of two particular levels or 'horizons' of black limestones interstratified with dark shales. Beushausen (1900)

* Corresponding author. Fax: +32-2-6477359.
E-mail address: xdevlees@ibelgique.com

PII: S0031-0182(01)00478-3

originally grouped these levels in one unit (the 'Kellwasser-Kalk'). Schindewolf (1922) and Schmidt (1928) recognised a Lower and an Upper Kellwasser Horizon (LKK and UKK). In the last few years, the UKK has attracted considerable attention among those geologists and palaeontologists concerned with Devonian stratigraphy and global events. This horizon is closely connected with a global bioevent corresponding to a major faunal change and gave rise to the partition of the Upper Devonian into two geological stages, namely the Frasnian and the Famennian. This faunal change at the top of the Frasnian is known as the 'Kellwasser Event' (Walliser, 1980, 1984) and is characterised by stepwise extinctions (Sandberg et al., 1988; Walliser et al., 1988).

The top of the UKK corresponds to stratigraphic boundary level as suggested by Walliser et al. (1989). Numerous sections comprising both horizons (LKK and UKK) are known in Germany (Buggisch, 1972, 1991). The Steinbruch Schmidt section is particularly well exposed and was proposed as a candidate for the GSSP (global stratotype and section point) by Walliser (1988). This section, situated 750 m NE of Braunau near Bad Wildungen in the Ense area of the Kellerwald, in the eastern part of the Rheinisches Schiefergebirge (Fig. 1), comprises a cephalopod-bearing limestone sequence ranging in time from the Early *rhenana* up to the *rhomboidea* conodont Zones. The two dark Kellwasser Horizons are intercalated in a light grey carbonate sequence. Faunal evolution and lithology of the Steinbruch Schmidt section have been studied in detail by Walliser et al. (1989), Ziegler and Sandberg (1990), Schindler (1990a,b, 1993), Feist and Schindler (1994) and Casier and Lethiers (1998). This section has also been studied by Goodfellow et al. (1988) who found trace element enrichment around the boundary, possibly related to a facies change from strongly anoxic conditions below the F/F boundary to less reduced conditions above the boundary. They also documented a positive enrichment in $\delta^{13}C$ in the UKK. Later, Joachimski and Buggisch (1993, 1996) and Joachimski et al. (1994) reported two positive carbon isotope excursions at Schmidt and other F/F boundary sections in Central Europe. These isotopic excursions coincide with the Kellwasser Horizons and indicate two phases of enhanced burial of organic carbon. In addition, the formation of the Kellwasser Horizons seems linked with short-term transgressive–regressive (T–R) pulses superimposed on a global eustatic highstand (Johnson et al., 1985; Sandberg et al., 1988; Buggisch, 1991). Similarity of the $\delta^{13}C$ curve between all these sections indicates several changes in the oceanic carbon reservoir during the late Frasnian.

All the cited papers concern mainly the faunal distributions of various groups around the boundary or geochemical analyses. A few (McGhee et al., 1986; Goodfellow et al., 1988) were devoted to the search for a possible extraterrestrial cause for this Upper Devonian mass extinction. As the extraterrestrial origin cannot be proved so far (McGhee et al., 1986), a more common geological phenomenon (sea-level variations, climatic oscillations, anoxic conditions) has been suggested by Joachimski and Buggisch (1993, 1996) to explain this major faunal change. To this end, we have carried out a sedimentological study of the Steinbruch Schmidt section in order to get detailed information on the eustatic variations and related phenomena associated with the F/F boundary.

2. Regional setting

The Frasnian is a period that records widespread carbonate platform drowning with an abrupt onset of condensed pelagic sedimentation in Europe (Wendt et al., 1984). Eustatic sea-level rises and tectonically controlled changes in palaeogeography related to rifting phases have been invoked by Schlager (1981) for this period. The Upper Devonian record of the German Rhenohercynian Zone illustrates these changes: condensed cephalopod limestones overlie submerged reefs or shallow-water platforms and volcanic rises. The Steinbruch Schmidt series was deposited on such a submarine rise (Fig. 1), below wave base level. Deeper basins (Meischner, 1971; Buggisch, 1972) flank the studied section to the NW and the SE.

The Upper Devonian palaeogeography of the Rheinisches Schiefergebirge consists of a mixed

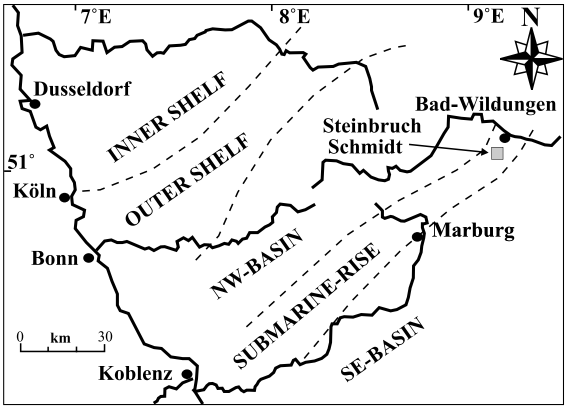

Fig. 1. Palaeogeographic map of the western part of the Rheinisches Schiefergebirge with localisation of the Steinbruch Schmidt section. Late Devonian marine palaeoenvironmental reconstitution from Meischner (1971).

siliciclastic–carbonate shelf bordering the Old Red Continent to the south. Limestones, marls and shales were deposited in adjacent epicontinental basins. Reefal and condensed pelagic cephalopod limestones were formed on submarine topographic elevations that originated either as tectonic fault-bounded rises or as volcanic seamounts (Krebs, 1979). Nodular limestones intercalated with shales containing slumps are present on the slopes of these rises, whereas shales with turbiditic siltstones and sandstones dominate basins.

3. Microfacies analysis

One hundred and fifteen samples have been collected through the condensed (9 m-thick) Steinbruch Schmidt section (Fig. 2). The bioclast abundance as well as the sedimentary structures (observed in thin sections) have been systematically studied (Fig. 2).

The petrographic study allows the recognition of three major microfacies (MF1 to MF3) subdivided into several lithotypes according to their fossil content and sedimentary structures. The microfacies succession (from 1 to 3) constitutes the standard sequence of the series and records a shallowing evolution from quiet environments below the storm wave base level to more energetic environments near this level.

3.1. Microfacies 1 (MF1): basinal environments

(a) MF1a: dark laminated mudstones and mudshales poor in marine fauna (Plate IA)

This microfacies is characterised by a poor faunal content consisting of small molluscan shells mixed with rare radiolarians, ostracods and tentaculitids. The well-laminated structure consists of an alternation of dark laminae (up to 1 mm thick) enriched in organic compounds and lighter laminae (millimetres to centimetres thick). The clastic minerals are composed of abundant silty quartzose grains (<60 μm) and white micas (<100 μm). No burrowing is observed.

(b) MF1b: dark laminated bioclastic packstones (Plate IB)

These correspond to densely packed and laminated packstones with abundant molluscs (goniatites and bivalves), tentaculitids, ostracods and a few radiolarians embedded in a micritic and dolomitised matrix rich in organic compounds. The laminar structure is formed by the alternation of rich bioclastic laminae (up to 2 cm thick) and mud laminae (1 mm to 1 cm thick) displaying a poorer faunal content. The clastic materials are the same as for MF1a. No bioturbation features have been observed.

(c) Interpretation: MF1 occurs mainly in the Kellwasser Horizons (Fig. 3) and is the deepest microfacies of the section. This mud-supported microfacies displays a well-preserved laminated structure and contains (MF1b) abundant pelagic fossils, such as goniatites, tentaculitids and radiolarians. These characteristics, as well as the abundance of organic compounds, suggest an environment of relatively deep, quiet and poorly oxygenated water in the aphotic zone. The inferred depth is below significant storm wave or current activity, i.e. >200 m by comparison with the Recent (Reineck and Singh, 1975; Guillocheau and Hoffert, 1988) or with the palaeoenvironmental reconstruction of the Coumiac series in the Upper Frasnian of southern France (Préat et al., 1998).

In such environments the dominant sedimentary process is decantation from suspended matter. Single ostracod shells, oriented 'convex-down', also support the interpretation of a quiet sedimen-

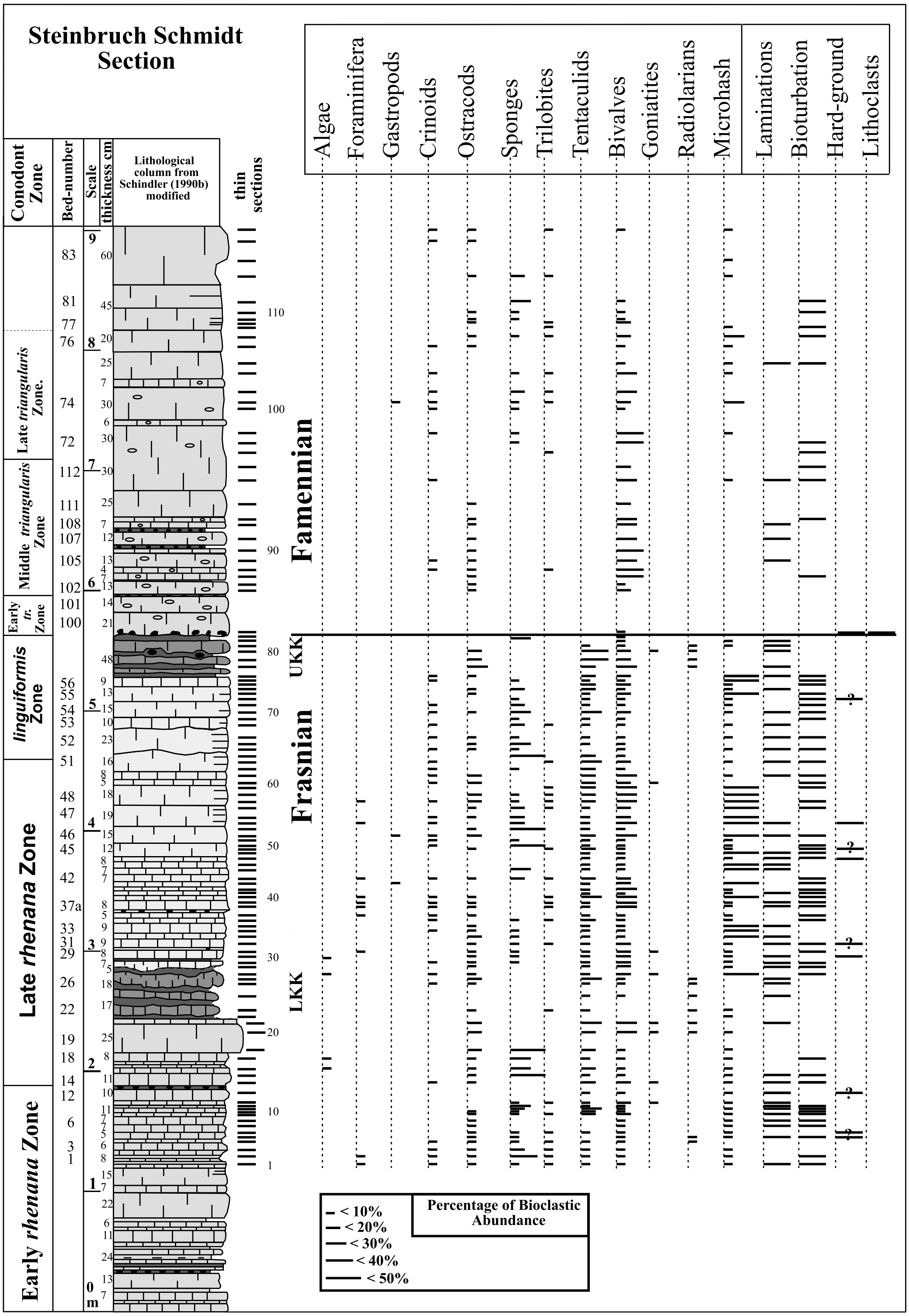
Steinbruch Schmidt Section
Conodont Zone
Bed-number
Scale thickness cm
Lithological column from Schindler (1990b) modified
thin sections
Early rhenana Zone
Late rhenana Zone
linguiformis Zone
Early tr. Zone
Middle triangularis Zone
Late triangularis Zone.
Frasnian
Famennian
LKK
UKK
Algae
Foraminifera
Gastropods
Crinoids
Ostracods
Sponges
Trilobites
Tentaculids
Bivalves
Goniatites
Radiolarians
Microhash
Laminations
Bioturbation
Hard-ground
Lithoclasts
Percentage of Bioclastic Abundance
< 10%
< 20%
< 30%
< 40%
< 50%

tation (Guernet and Lethiers, 1989). The well-preserved laminated fabric is explained by the absence of benthonic activity due to anoxic conditions. Our interpretation is similar to the one of Buggisch (1972) for whom the Kellwasser Horizons were deposited under sapropelic conditions as indicated by the absence of current activity and benthos, abundant organic compounds and the enrichment in Cu.

3.2. Microfacies 2 (MF2): hemipelagic/outer distal ramp sponge environments

(a) Microfacies 2a (MF2a): bioclastic and bioturbated mudstones and wackestones

This microfacies constitutes a transition between microfacies 1b and 2b. The faunal content is poor and composed of a few sponge spicules, ostracods, molluscan shells and scarce radiolarians. The micritic matrix is slightly recrystallised to a calcite microsparite. Laminated structure is poorly preserved as a consequence of burrowing activity.

(b) Microfacies 2b (MF2b): sponge wackestones and bafflestones (Plate IC,D)

Sponge wackestones and bafflestones are composed of abundant centimetre-sized sponge nodules with connected spicules, associated with a few bioclasts (ostracods, crinoids or trilobites). Laminated microbioclastic layers (<1 cm) rich in tentaculitids, molluscs (gastropods and bivalves), ostracods, crinoids, trilobites, foraminifers (*Frondilina*, *Tikhinella*) and poorly preserved algal fragments of kamaenids and *Rectangulina* Antropov 1959 (Mamet and Roux, 1975) are occasionally present. Small-sized peloids are also associated. The molluscan and crinoidal fragments display perforations that are probably sponge borings. The microbioclastic layers present an erosive base and a plane-parallel top surface. Numerous thin (<1 mm) irregular stromatactoid cavities (sensu Boulvain, 1993) with geopetal infillings, are present in the matrix. This facies displays a typical nodular fabric due to the sponge nodules. Pressure solution processes (stylolites), particularly marked around the sponge nodules, accentuate this fabric. Bioturbation is weakly developed.

Rare bored hardgrounds are present and the two best preserved are located immediately above the Kellwasser Horizons. The oldest one, above the LKK, shows (Plate IID–F) an irregular surface, with encrusted sponges and goniatite shells. The surface is perforated by nearly horizontal (centimetres in length) and vertical (1 or 2 mm in size) borings filled with the overlying sediments (MF2). Immediately above this surface, another surface encrusted with Fe-hydroxide coatings is present and indicates a second interruption of the sedimentation rate. The youngest hardground, located just above the F/F boundary (Plate IIC), correspond to a microbreccia composed of subrounded and subangular sponge mudstone nodules (<1 cm) embedded in a microbioclastic wackestone with a few molluscans and ostracods.

(c) Microfacies 2c (MF2c): laminated microbioclastic stromatactoid wackestones (Plate IE,F)

These micritic and microsparitic wackestones contain a few irregular cavities (<1 mm in size) of stromatactoid aspect with geopetal infillings of dense micropeloidal mudstones with thin molluscs and ostracods. The matrix is rich in microbioclasts with abundant tentaculitids (only in the Frasnian part), few molluscs, ostracods, trilobites and crinoids.

(d) Interpretation: MF2 records the development of nodular and layered sponges culminating in the bafflestones of microfacies 2b. Millimetre- to centimetre-thick microbioclastic layers are interstratified within the sponge sediments. They contain several fossils (foraminifers and algal fragments) coming from a distant shelf. Their erosive bases (MF2b and 2c) are indicative of episodic higher-energy conditions suggesting distal

Fig. 2. Lithological column and bed number from Schindler (1990a,b), conodont zones from Feist and Schindler (1994). Thin-section position, bed thickness, fossil abundance and sedimentary structures are noted in front of the lithological column. Note that algae, foraminifers, goniatites and radiolarians temporarily disappear at the F/F boundary. The sponges disappear in both Kellwasser Horizons (i.e. LKK and UKK).

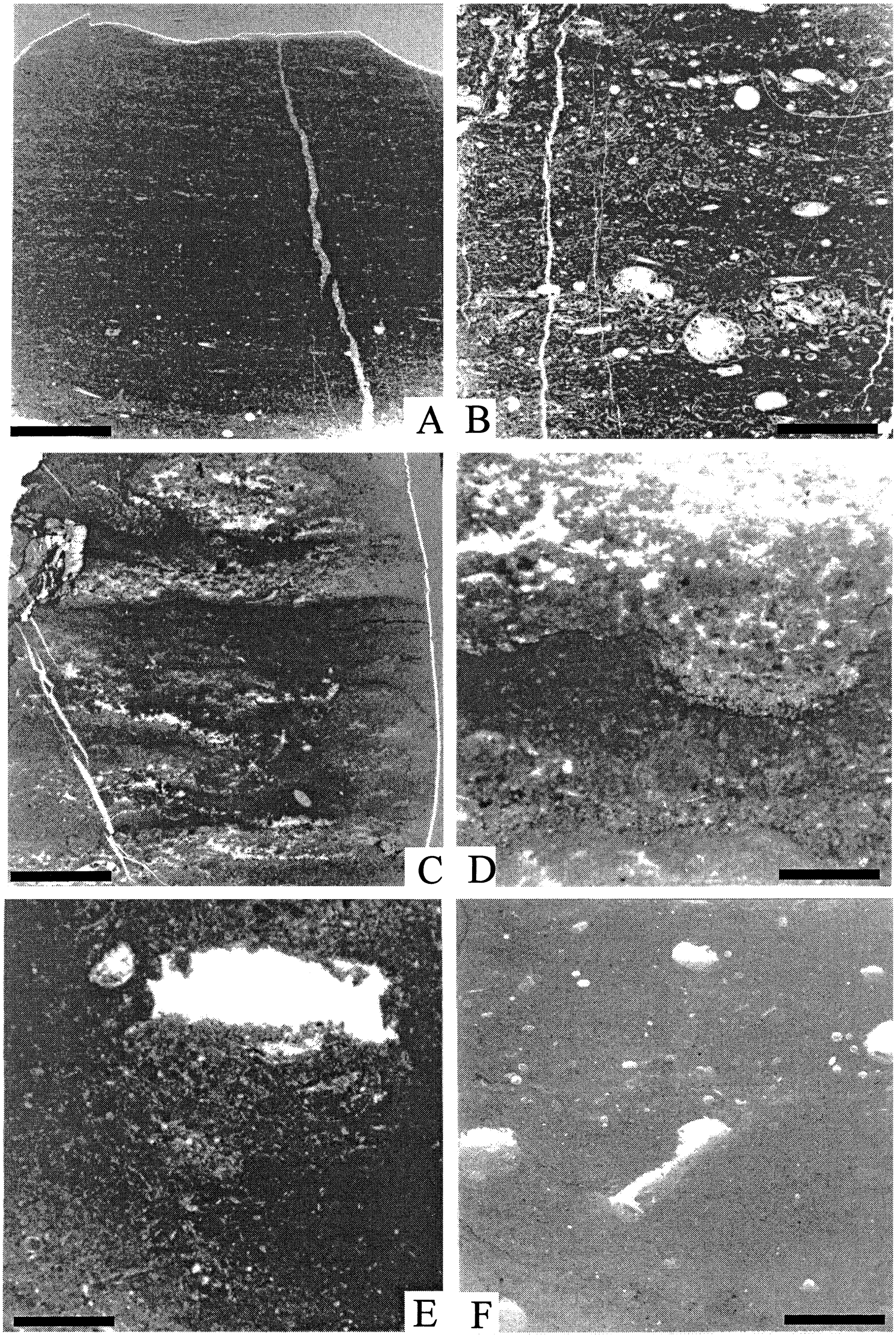
A
B
C
D
E
F

tempestites (sensu Aigner, 1985) or turbidites. The succession of these three lithotypes suggests a distal–proximal gradient as stromatactoid cavities (sensu Bourque and Boulvain, 1993) and microbioclastic layers increase from MF2a to MF2c. This evolution records a decrease of depth along a distal ramp. The same features have been recognised in the Upper Devonian of the Coumiac stratotype section (Montagne Noire, France) as interpreted by Préat et al. (1998).

3.3. Microfacies 3 (MF3): outer ramp close to the storm wave base

(a) MF 3a: laminated microbioclastic packstones (Plate IIA)

The biogenic fraction consists of microbioclasts of tentaculitids, molluscs (gastropods and bivalves), ostracods, crinoids, foraminifers, trilobites and poorly preserved algal fragments. Small-sized peloids are present. The layers (millimetres to several centimetres thick) show wavy laminations, erosive bases and grading. The sediment contains scarce perforated hardgrounds filled with peloidal and microbioclastic wackestones. Rare stromatactoid cavities are present.

(b) Microfacies 3b (MF3b): coarse-grained bioclastic packstones (Plate IIB)

The microfacies is similar to the previous one but the layers are thicker (several centimetres) and show a coarser texture due to large shells (molluscs). The layers are enriched in tentaculitids or in molluscs. Only a few crinoids and ostracods are present.

(c) Interpretation: The MF3 shows a distinct thickness increase (relative to MF2) of the microbioclastic layers, of bioclast size, some grading and frequent erosive base layers. These characteristics suggest more energetic conditions near the storm wave base, and related to turbiditic or storm processes (sensu Aigner, 1985).

4. Sedimentary model and microfacies evolution

4.1. Sedimentary model

Despite the difficulty in establishing a bathymetric sequence (condensed series), the order of the microfacies sequence is established using mostly sedimentological criteria, e.g. bioclastic laminations, graded bedding and granulometry. The increase in bed thickness suggests a distal–proximal gradient from MF1 to MF3. The sequential evolution records a 'shallowing-upward' trend from deep, quiet and poorly oxygenated environments, below the storm wave base, to more energetic environments influenced by current activity around the storm wave base. All the microfacies are below the photic zone as indicated by the absence of in situ algae. Mudshales, mudstones and wackestones suggesting a quiet and autochthonous sedimentation dominate the sediments. Microbioclastic packstone layers are occasionally interstratified in the sediments and are related to turbiditic or storm-induced currents. Pelagic or nektonic fossils (tentaculitids, ammonoids, radiolarians) are mainly associated with MF1. The benthonic fauna is represented by the sponges of the MF2 and the crinoids of

Plate I. Pictures illustrating the F/F microfacies of the Steinbruch Schmidt section. (A) MF1a: laminated mudstone and black mudshale. Small molluscans, radiolarians and ostracods only are present. The laminated structure consists of an alternation of black laminae (up to 1 mm thick) rich in organic compounds and lighter laminae (from 1 mm to 1 cm). Sample SQ25, scale bar = 0.5 cm. (B) MF1b: black and laminated bioclastic packstone (abundant goniatites and bivalves, tentaculitids, ostracods and rare radiolarians). No bioturbation features. Sample SQ22, scale bar = 0.5 cm. (C) MF2b: wackestone and bafflestone with centimetric sponge nodules associated with bioclasts consisting of a few ostracods, crinoids and trilobites. Sample SQ17, scale bar = 0.5 cm. (D) MF2b: wackestone and sponge bafflestone. The picture shows a small discontinuity surface surmounted by sponges (light layers). Sample SQ45, scale bar = 0.5 cm. (E) MF2c: laminated and microbioclastic wackestone with stromatactoidal cavities. The close view of one of these cavities shows the geopetal filling consisting of a fine and dense micropeloidal matrix with few ostracods. Sample SQ4, scale bar = 1 mm. (F) MF2c: laminated and microbioclastic wackestone with few irregular cavities of stromatactoidal aspect (below 1 mm in size). The geopetal infilling corresponds to a micropeloidal-rich mudstone with rare ostracods and molluscs. Sample SQ4, scale bar = 0.5 cm.

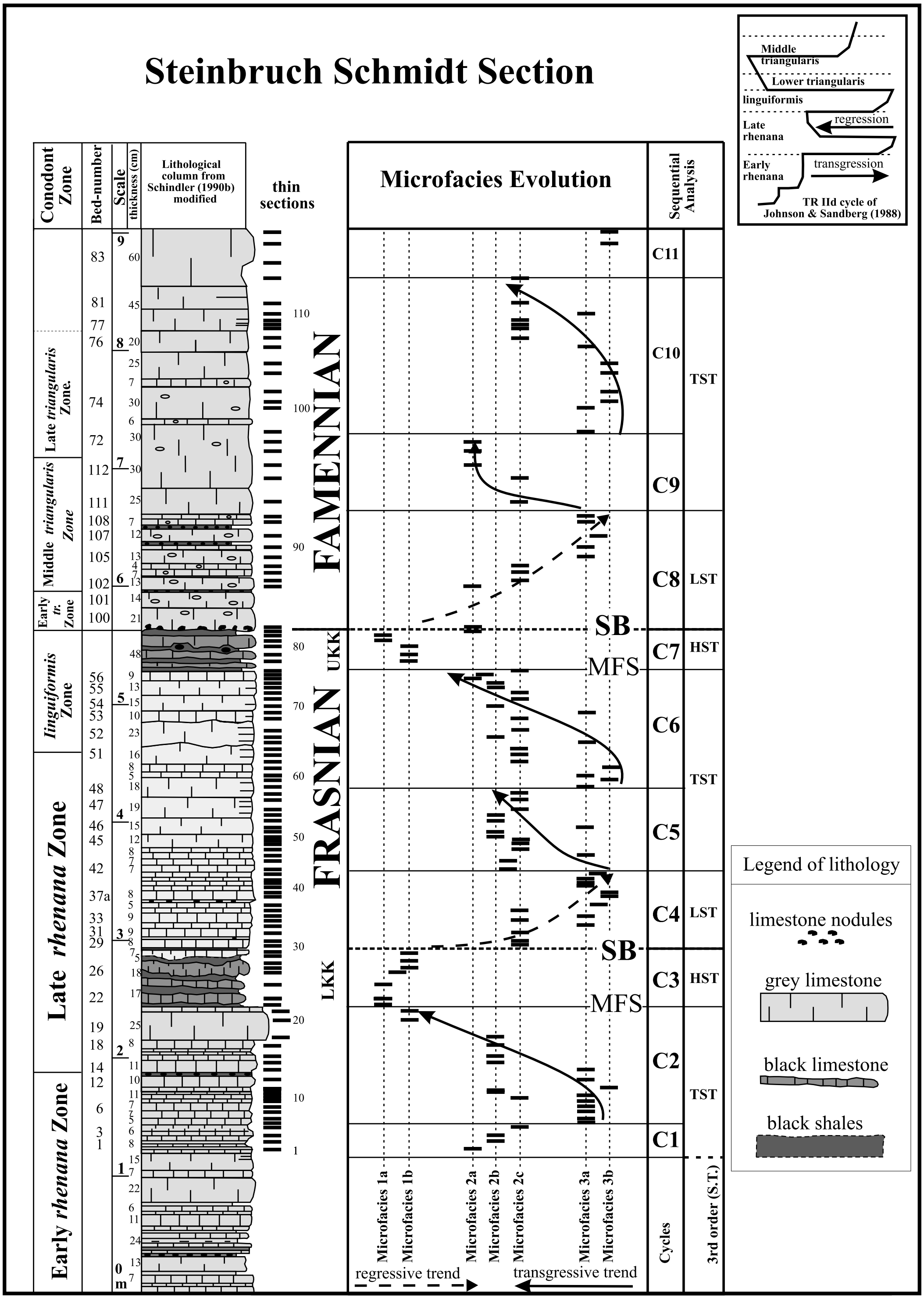

Fig. 3. Microfacies evolution and sequential stratigraphy of the F/F boundary series (fourth- and third-order cycles) are noted in front of the lithological column. The T–R IId cycle of Johnson and Sandberg (1988) is also schematised. S.T. = systems tract, LST = lowstand systems tract, TST = transgressive systems tract, HST = highstand systems tract, SB = sequence boundary.

the MF3, the latter being probably derived from the destruction of distant crinoidal meadows.

According to these characteristics, the deepest sediments are mudshales and laminated bioclastic mudstones of MF1. They correspond to the black shale facies of the Kellwasser Horizons that were therefore deposited below the storm wave base. From this deep environment a progressive transition leads to the sponge microfacies (MF2) which are progressively interstratified with fine laminated microbioclastic packstones. The origin of the distal calcareous tempestites or turbidites is probably linked during Late Devonian times to a distant shelf located in NW Germany (Fig. 1).

In summary, our microfacies analysis indicates a general open marine environment close to the storm wave base. The inferred depth could be around 200 m (Friedman and Sanders, 1978; Guillocheau and Hoffert, 1988) and could fit the palaeogeographic setting of the Steinbruch Schmidt section located on a submarine rise overlying a volcanic basement (Meischner, 1971; Buggisch, 1972). This situation could explain the relative homogeneity of the facies (only three different microfacies are present), sea-level variations being unable to affect greatly the depositional environments at this inferred depth.

Pelagic sedimentation on ancient submarine rises differs both from actively productive carbonate platforms and from deep-sea basins. Bottom currents prevent the deposition of planktonic organisms (such as radiolarians) promoting instead a preferential accumulation in adjacent basins (Baumgartner, 1987, 1990). Such a situation is observed at Steinbruch Schmidt where radiolarians are scarce and only present in microfacies MF1. Martire (1992) also invoked a depth of hundreds of metres for condensed facies developed in submarine rises in the Jurassic (Rosso Ammonitico) of NE Italy.

4.2. Pelagic sedimentation and sequential analysis

In the context of condensed facies on a drowned platform, Martire (1992) has shown that the onset of sedimentation occurs during the transgressive and highstand systems tracts when the current activity is reduced allowing pelagic sediments to fall towards the bottom. The sequence boundaries are correlated with stratigraphic gaps, and their associated erosional submarine surfaces are frequently indicated by Fe (–Mn) hardgrounds. They are ascribed to the accentuation of ocean circulation induced by sea-level falls and thus with the lowstand systems tract (LST) (Martire, 1992).

The Steinbruch Schmidt microfacies evolution (Fig. 3) shows a small-scale rhythmicity composed of sub-metre-scale transgressive and regressive cycles. The Kellwasser Horizons do not present any sequential evolution, the facies record persistent deep-water environments. Eleven cycles are recognised (C1–C11; Fig. 3) and their thickness ranges from 0.4 m to 1.4 m. These cycles do not exhibit any clear thickening (or thinning) upward pattern, their individual beds being decimetre thick. The boundaries between the beds show numerous omission surfaces (millimetric argillaceous joints) of probably important time range as suggested by the conodont zonation. Fig. 3 shows that one conodont Zone contains from less than one a cycle up to five cycles, indicating the importance of the condensation of the series. In such a situation, it is impossible to recognise low-level ordering of the sequences sensu Van Wagoner et al. (1988). The presence of two hardground levels above each Kellwasser Horizon confirms the importance of the condensation of the series. The upper hardground level (5 cm thick) is located just above the F/F boundary and contains abundant nodular sponges in a bioclastic micritic matrix. The second hardground level (millimetre thick) lies just above the LKK (Plate IID–F) and shows vertical burrows 1 or 2 mm deep which are sometimes nearly horizontal (1 cm long) and filled with the MF2 sediments.

4.3. Discussion

The upper hardground corresponds to the 'brecciated layer' interpreted by Sandberg et al. (1988) and Schindler (1993) respectively as a high energy event (storm deposit?) or as "an in situ generation due to the different consistency of the limestone compared with the Kellwasser sediments during lithification". This layer can be

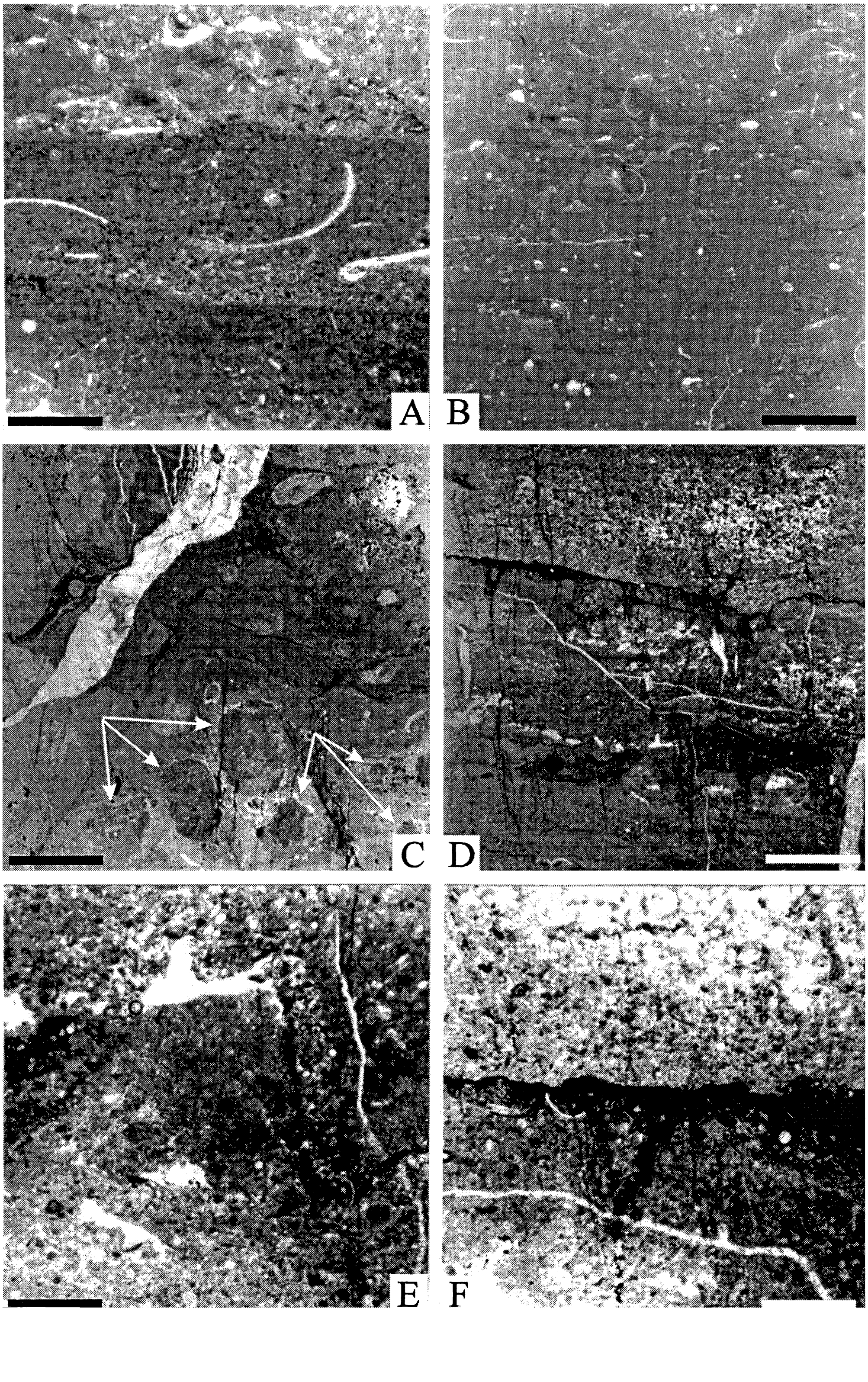

A
B
C
D
E
F

traced as a distinct marker horizon due to its regionally wide distribution (Schindler, 1993). In our view, these nodules represent an initial sponge layer (bafflestone) which has been intensively bored during extremely reduced sedimentation. The layer is fragmented and transformed into small blocks that have been reworked and incorporated in the overlying sediments (MF3). This process leads to the formation of a breccia layer composed of subrounded to subangular (less than centimetre-sized) nodules (Plate IIC). Similar processes have been described in the Coumiac section by Préat et al. (1998) in the same stratigraphic interval. The formation of this 'breccia' implies a time gap as suggested by the Lower *triangularis* conodont Zone which is the most reduced biozone of this section (Fig. 3). Each of these hardground levels is followed by a regressive pattern in the sedimentation (Fig. 3) and could therefore correspond to two third-order sequence boundaries sensu Van Wagoner et al. (1988). The sequence boundaries are also similar to those reported by Martire (1992) from the pelagic series of the Rosso Ammonitico. One of these sequences is complete in the Steinbruch Schmidt section (i.e. from C4 to C7, Fig. 3) and encompasses nearly two conodont zones. This sequence is well within the third-order time range reported in the literature (see for example Einsele et al., 1991). The vertical stacking of 11 cycles and the presence of two sequence boundaries make it possible to describe third-order evolution of the sedimentation. A succession of seven systems tracts has been established: cycles C2, C5–6, C9–10 belong to a transgressive systems tract (TST), and the two Kellwasser Horizons to a highstand systems tract (HST). The LST is defined by cycles C4 and C8 showing a shallowing-upward succession from MF1 to MF3.

The generation of the black sediments (shales and limestones of the Kellwasser Horizons) is thought to be due to vertical oscillations of O_2-deficient water masses, i.e. episodic rises of the anoxic layer (Schindler, 1990a). The sudden income of bivalves and icriodontids within the UKK can be explained by an even slight shift towards more oxygen content, but still in the dysaerobic zone. Such a process is more likely than a sudden sea-level fall (Walliser et al., 1988). The LKK and UKK are certainly related to the income of anoxic bottom water conditions that have also favoured the development of opportunistic and adapted species to O_2-depleted water. We have to ask if the vertical oscillations of the anoxic layer correspond to a mechanism driven by sea-level fluctuations or not. In fact, the mechanism of sea-level fluctuations seems to explain all the observations reported here from the microfacies study. Moreover, the sequential model proposed here is compared with some recent papers as well as with the evolution of the conodont biofacies (see below).

A comparison between the evolution of the Steinbruch Schmidt microfacies evolution and the sea-level curve (T–R cycle IId) of Johnson et al. (1985) and Johnson and Sandberg (1988) shows similar trends at a large scale, but some discrepancies in detail (Fig. 3). The transgressive episodes of the basal part of the Upper *rhenana* and the uppermost part of the *linguiformis* cono-

---

Plate II. Pictures illustrate the F/F microfacies of the Steinbruch Schmidt section. (A) MF3a: microbioclastic packstone containing tentaculitids, molluscs (gastropods and bivalves), ostracods, crinoids, trilobites as well as foraminifers and algal fragments (not visible on the picture). The microbioclastic layers (millimetres to centimetres thick) alternate with thin millimetric layers of argillaceous mudstone. They present an undulating structure, erosive bases and sometimes a grading. Sample SQ6, scale bar = 0.5 cm. (B) MF3b: bioclastic packstone rich in bivalves and ostracods. The thickness of the layers reaches several centimetres. Sample SQ89, scale bar = 0.5 cm. (C) The upper hardground level, at the base of the Famennian, corresponds to a microbreccia of subangular and centimetric nodules of sponge mudstones. These nodules are embedded in a microbioclastic wackestone with molluscs and ostracods. Sample SQ84, scale bar = 0.5 cm. (D) The lower hardground level, above the LKK, shows an irregular surface encrusted by sponges and goniatites. This surface is perforated by vertical (1–2 mm deep) and centimetric sub-horizontal burrows and filled by sediments of microfacies MF2c. A second hardground level underlined by a ferruginous surface (Fe–Mn) surmounts this first surface and the fillings. Sample SQ30, scale bar = 0.5 cm. (E) The photo shows a perforated surface by vertical burrows of 1–2 mm deep. Sample SQ30, scale bar = 1 mm. (F) Close view on the condensed surface underlined by Fe–Mn? coatings. Sample SQ30, scale bar = 0.5 cm.

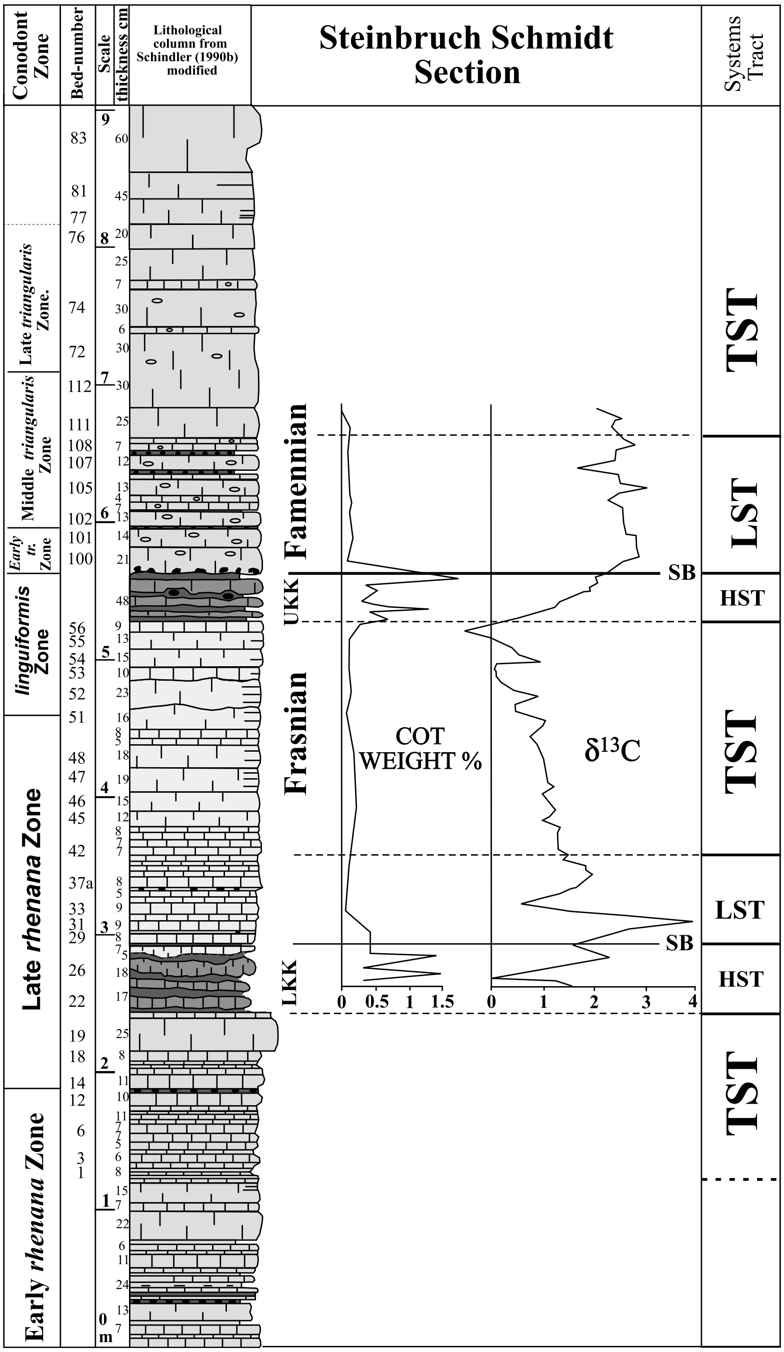

Fig. 4. Comparison between the sequential model and carbon isotope (Joachimski and Buggisch, 1993) as well as TOC (Casier et al., 1999) results. Each Kellwasser records the highest TOC values during highstand conditions and the highest $\delta^{13}C$ values at the base of LSTs.

dont Zones correspond to the two Kellwasser Horizons. As we have seen previously at the Steinbruch Schmidt section, the transgressions started below the Kellwasser Horizons, which represent only eustatic highstands in our interpretation (Fig. 3). In both cases, a regressive episode starts at the end of the Kellwasser Horizons, the second one, at the base of the Famennian, being of greater amplitude than shown on the curve of Johnson et al. (1985). Due to the significant depth in the Steinbruch Schmidt series the importance of these eustatic changes is difficult to highlight. For example, the TST/HST boundary corresponding to the maximum flooding surface (MFS) is not easily found in such condensed sequences. Schindler (1993) has reported that a characteristic layer immediately below the UKK shows a distinct enrichment of various faunal elements such as trilobites, ostracods, cricoconarids and goniatites, each of these groups also displaying an increased numbers of specimens. This layer, which is also recognised in other German sections by Schindler (1993), corresponds in our sequential model to the TST/HST transition (MFS). Such a layer with a marked enrichment in fossils seems to be not present below the LKK.

From several sections in Europe, two positive carbon isotope excursions have been recognised in the Kellwasser Horizons by Joachimski and Buggisch (1993). The carbon isotope pattern indicates two phases of enhanced burial of organic carbon. In addition, the formation of the Kellwasser Horizons seems to be linked with short-term T–R pulses superimposed on a global eustatic highstand (Johnson et al., 1985; Sandberg et al., 1988; Buggisch, 1991). These isotopic excursions have been related to the development of anoxic events. The eustatic pattern proposed in this paper indicate that each Kellwasser Horizon correspond to a third-order HST. The end of the Frasnian is superimposed on a second-order highstand, corresponding to the maximum sea-level highstand known in the Devonian, which occurs at the F/F boundary (Johnson and Sandberg, 1988). In fact, a comparison has been made here between the systems tracts succession and carbon isotope (Joachimski and Buggisch, 1993) as well as TOC (total organic carbon; Casier et al., 1999) results. Each Kellwasser records the highest TOC values during highstand conditions. Looking in details at the carbon isotope curve of Steinbruch Schmidt (Fig. 4), a $\delta^{13}C$ peak is recorded just above the LKK at the base of the LST. The $\delta^{13}C$ values decrease from the end of the LST to the lowest values below the UKK in the TST. From that point, $\delta^{13}C$ values increase again during the UKK up to the basal Famennian (LST). These observations indicate that the highest $\delta^{13}C$ values are recorded in each case at the base of LSTs and that $\delta^{13}C$ values decrease between the Kellwasser Horizons from the LST up to the end of the TST. Eustatic fluctuations are clearly correlated with the $\delta^{13}C$ isotopic curve and could partially explain the fluctuations of the inorganic carbon isotope curve.

Recently, a synthesis of these upper Frasnian eustatic variations in shallow marine environments has been documented in Belgium and South China by Muchez et al. (1996). In both areas two sequence boundaries were suggested, the first one occurring in the Upper *rhenana* Zone and the second one around the F/F boundary at the top of the *linguiformis* Zone. The storm deposits above these sequence boundaries are interpreted as lowstand deposits. Therefore similar F/F boundary third-order eustatic variations are documented in both shallow and deep environments.

The Steinbruch Schmidt section has been studied for conodonts by Sandberg et al. (1988) who indicate several biofacies changes around the F/F boundary. The late Frasnian (before and during the UKK) is characterised by a palmatolepid–polygnathid biofacies suggesting a deposition depth of 100 m or more (Sandberg et al., 1997). All conodonts of the Early and Middle *triangularis* zones compose a mixed palmatolepid (deep)–icriodid (shallow) biofacies indicating a depth ranging from more than 100 m to 60 m (Sandberg et al., 1997). This biofacies change records an eustatic fall at the F/F boundary. Sandberg et al. (1988) interpreted the first increase of *Icriodus* in the UKK as the beginning of the eustatic fall and the gradual increase upwards of *Icriodus* at the end of the UKK as an increased shallowing event. From our view, the eustatic fall, revealed by the

Table 1
Sample identification (according to thin-section numbers of Figs. 2 and 3), clay mineralogy and illite composition of the clay fraction of Steinbruch Schmidt section (F/F boundary)

Sample	I (%)	K (%)	M (%)	C (%)	Qz	F.K.	Goeth	IC cal	Esq (g)	001/002	IR	W1 (g)	W2 (g)
SQ1	50	50			?		?	0.43	0.38	2.6	0.87	0.3	0.35
SQ8	60	40			P			0.34	0.37	2.7	1.17	0.25	0.28
SQ15	60	40			P			0.43	0.46	2.18	1.1	0.3	0.3
SQ21	70	25	5		P		P	0.465	0.3	3.38	1.23	0.32	0.6
SQ22	75	20	5		P		P	0.62	0.43	2.32	1.33	0.41	0.42
SQ25	75	15	10		?		P	0.4	0.4	2.5	1.43	0.28	0.4
SQ30	70	25	5		P		?	0.5	0.5	2.02	0.85	0.34	0.34
SQ31	65	35			P			0.43	0.42	2.36	1.27	0.3	0.3
SQ38	55	40		5	P			0.43	0.32	3.14	1.29	0.3	0.3
SQ42	50	45		5	P		?	0.43	0.42	2.38	1.41	0.35	0.35
SQ44	70		30		P	P			0.41	2.43	1.98		
SQ45	55	45			P		P	0.465	0.42	2.39	1.27	0.32	0.3
SQ55	60	35		5	P			0.43	0.33	3	1.31	0.3	0.35
SQ63	65	35			P	P	P	0.43	0.48	2.09	1.23	0.3	0.32
SQ71	70	30				P	P	0.43	0.46	2.18	1.22	0.3	0.31
SQ78	80	20			P		P	0.6	0.47	2.16	1.42	0.4	0.3
SQ80	90	10				P	P	0.48	0.4	2.5	1.51	0.33	0.3
SQ84	90	10			P	P		0.515	0.37	2.69	1.15	0.35	0.32
SQ84b	75	25				P	P	0.45	0.42	2.37	1.58	0.31	0.35
SQ90	65	35			P	P	P	0.43	0.38	2.63	1.42	0.3	0.32
SQ91	65	35			P		?	0.515	0.38	2.62	1.32	0.35	0.4

Sample number, percentages of illite (I), kaolinite (K), mixed layers (M), chlorite (C), presence (P) of quartz (Qz), K-feldspaths (F.K.) and goethite (Goeth), calibrated illite crystallinity (IC cal), Esquevin index glycolated (Esq (g)), 001/002 ratio glycolated, IR index glycolated (IR) and Shirozu index W1 and W2 (glycolated).

transition from a highstand during the UKK to a lowstand at the base of the Famennian, is in good agreement with the conodont biofacies change. This sea-level change is underlined by the maximal abundance of *Icriodus* at the base of the Famennian. The shallowing event, linked with the *Icriodus* increase, at the end of the UKK could be interpreted as the early part of the eustatic fall according to the definition of a HST from Van Wagoner et al. (1988). These authors have subdivided the HST into three parts: the lower part indicates the end of the transgression, the middle part commonly consists of an eustatic stillstand and the late part corresponds to the beginning of the eustatic fall. Thus the late part of the highstand records the beginning of the sea-level lowering. With such an explanation, the conodont biofacies change fits the sequential analysis well.

Detecting third-order eustatic variations through the F/F series in deep and condensed cephalopod limestone strata implies the recognition of the source process controlling these eustatic variations. Glacio- or tectono-eustatism could explain these sea-level variations. The recent paper of Streel et al. (2000), based on miospore analysis, concluded that violent volcanism might have caused long-term warming during the late Frasnian succeeded by a very short-term glacial phase in the Earliest Famennian. These authors argued that cooling and glaciation seem the most reasonable explanation for the major eustatic fall following the Kellwasser Event. Furthermore, Murphy et al. (2000) have proposed an eutrophication model based on carbon isotope and C:N:P atomic ratios of organic matter buried across the Kellwasser Horizons in Western New York State. Late Devonian climatic cooling and selective demise of taxa adapted to oligotrophic conditions are consistent with widespread and episodic eutrophication. Moreover, magnetic susceptibility measures made on several sections in

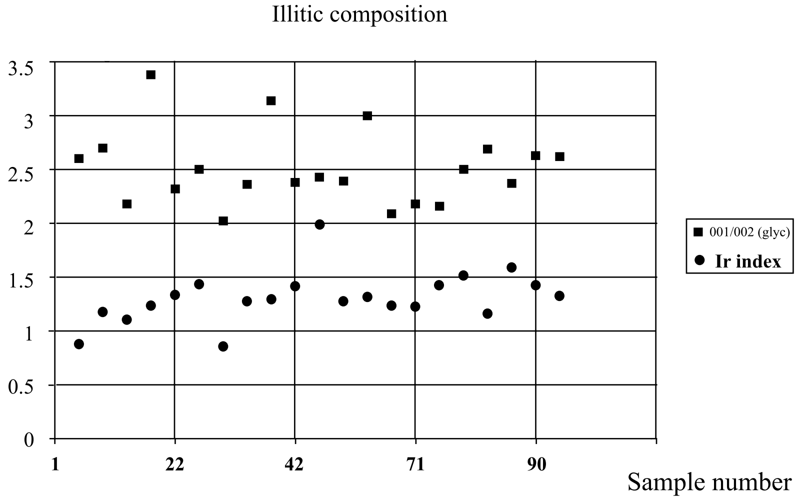

Fig. 5. Chemical composition of the illitic materials: the two parameters reveal a relatively high Fe content and the presence of interstratified illite–smectite materials. The x-axis corresponds to the sample number and the y-axis indicates the measure of the Ir index of Środoń (1984) and the measure of the 001/002 ratio for the illitic fraction.

Europe (Devleeschouwer, 1999) indicate a clear modification of the detrital input to the ocean, during the basal Famennian, linked to climatic or tectonic (orogenic surrection) changes. New multidisciplinary studies are needed to constrain precisely the eustatic-fluctuations model developed here as well as the source mechanism controlling sea-level variations.

5. Clay mineralogy

5.1. Sampling and methods

Twenty-one samples including different lithologies (limestones and shales) have been studied. The clay fraction (particles smaller than 2 μm) was separated by sedimentation after decarbonatation with HCl N/5 and defloculation with deionised water. X-ray diffraction analyses were carried out using a Philips PW1730 DX diffractometer with Cu–K radiation and performed on oriented pastes mounted on glass slides. Three X-rays diagrams were undertaken: under air-dried conditions, after saturation with ethylene glycol and after heating at 490°C for 2 h. Semi-quantitative determinations are based on the peak intensities and areas of selected clay mineral peaks (Holtzapffel, 1985). The heights of illite and kaolinite (001) peaks are taken as references.

The illite crystallinity (IC) values were determined by measuring the width of the (001) peak at half-height measured at $\pm 0.01°2\theta$ on oriented clay preparations after glycolation. The IC values obtained in the Laboratory of Sedimentology and Geodynamics at Lille 1 University (France) were corrected using several standard specimens allowing calibration with respect to IC international calibrated index (Warr and Rice, 1993, 1994). The crystallinity index standard (CIS) of Warr and Rice (1994) gives IC anchizonal limits of $0.25°\text{d}2\theta$ and $0.42°\text{d}2\theta$, which are the same as those of Kübler (1967). The chemical composition of the illitic materials was detailed using the methods of Esquevin (1969), Shirozu and Higashi (1972) and Środoń (1984) on glycol-saturated preparations.

5.2. Results

The clay assemblage is poorly diversified in the Steinbruch Schmidt section: clay minerals are dominated by illite (50–90%), kaolinite (10–50%), mixed layers (essentially 10–14s) (5–30%) and traces of chlorite (5%) (Fig. 9). Quartz, K-feldspar and goethite are also present (Table 1).

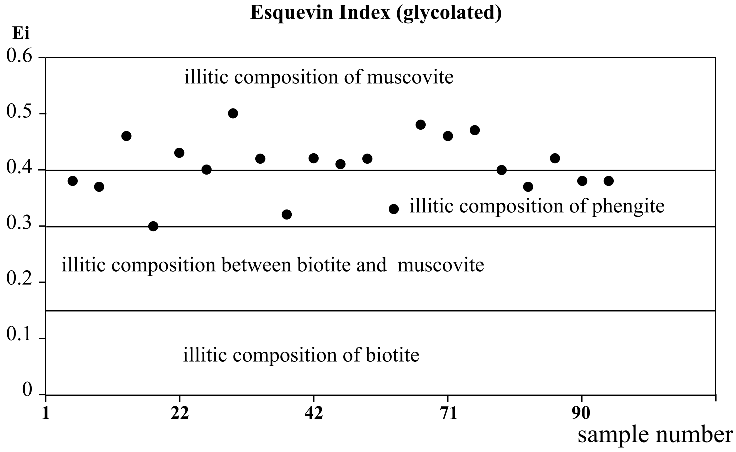

Fig. 6. Measure of the Esquevin index (Ei, *y*-axis) is reported for each analysed sample (*x*-axis). The results indicate a phengite to muscovite composition with Fe and Mg in the octahedral sheets (see text for more explanation).

5.2.1. *Illite*

The illites of the Steinbrich Schmidt section present large values of the 001/002 ratio (between 2.02 and 3.38) indicating a relatively high Fe content in the octahedral sheets (Fig. 5).

The Esquevin index (Ei, described by Kübler, 1968 and Esquevin, 1969) mean value (0.41) of the F/F boundary samples suggests a composition between muscovite and phengite revealing the presence of Fe and Mg in the octahedral sheets (Fig. 6).

The measure of the BB1 index of Środoń (1984) shows that F/F boundary samples indicate less than 15% of smectitic sheets in the interstratified illite–smectite and an ISII ordered type of interstratification.

Fig. 7 shows the IC values for clay samples: they present a relatively narrow range between 0.4 and 0.5 except for three values. Shirozu and Higashi's (1972) method has been followed, consisting in the measure of the half-height peak width for the 5-Å and 10-Å illite reflections and these are designated W2 and W1 respectively (Fig. 8). This method gives an estimation of the alter-

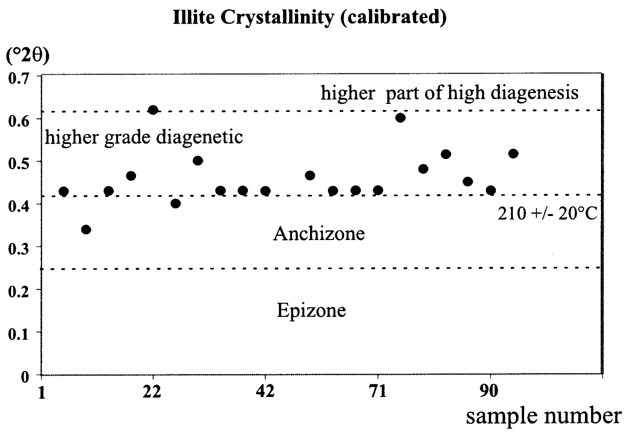

Fig. 7. Shirozu diagram build with W2 and W1 measures, (respectively *y*-axis and *x*-axis). The diagram indicates 'opened illite'. Only one sample had a high W1 value (SQ78) which is unfavourable to the measure of the illite crystallinity (see text for more explanation).

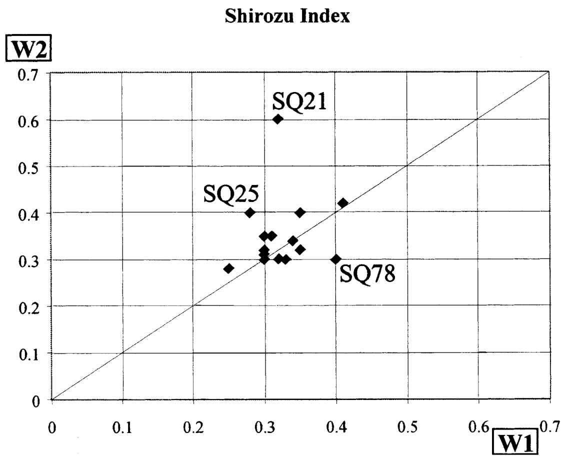

Fig. 8. The IC diagram reports the °2q values along the *y*-axis for each analysed sample (*x*-axis). Results indicate IC values near the diagenesis/anchizone boundary suggesting that the sediments have not reached low-grade metamorphism. Estimated temperatures are below 210 ± 20°C.

ation stage of illitic materials: when the W1 index is plotted along or close to the line with a 45° inclination angle the IC values are typical of 'well-crystalline' illites. As shown in Fig. 7, only sample SQ78 presents a W1 value larger than W2 indicating a more 'opened ' illite. Some samples show a W2 index higher than the average (for example SQ21 and SQ25) without affecting the measure of IC.

The illitic samples comprise a muscovite or phengite composition indicating a non-purely aluminous content. Moreover, a mixture of illite and interstratified illite–smectite with less than 15% of smectitic sheets and an ISII ordered type of interstratification is observed. A part or all of the illite could have experienced a diagenetic evolution as suggested by the BB1 values and the phengite composition. The detrital origin could not be totally avoided, as it is impossible to quantify the illite percentage coming from the diagenesis of terrigenous illites. Illite abundance is maximal during the two Kellwasser Horizons (Fig. 9) and varies gradually in the section.

5.2.2. Other clay minerals

Kaolinite, the second most abundant clay mineral, is particularly well represented (up to 50%) between the two Kellwasser Horizons (Fig. 9 and Table 1). Its percentage is lowest in the Kellwasser Horizons. Chlorite and mixed layers are only present as traces with the exception of sample SQ44 with 30% interstratified illite–smectite. Both minerals, occurring below the UKK and between the Kellwasser Horizons, suggest that no significant change in the clay composition occurred above the F/F boundary where only illite and kaolinites have been recorded. Sample SQ44, which shows an unusual clay mineralogy composed of illite and mixed layers, could indicate a bentonite layer (J.-F. Deconinck, personal communication) already described as such in Schindler (1990b).

5.3. Discussion

On the whole, IC values fall within the higher-grade diagenetic zone, near the diagenesis/anchizone boundary (Fig. 7). According to the Yang and Hesse (1991) subdivisions, the series has not reached low-grade metamorphism. Temperatures at the diagenesis/anchizone boundary, based on published values from the literature (Frey, 1987; Roberts et al., 1991; Warr, 1996; Garcia-Lopez et al., 1997; Han et al., 2000), seem to range between 200 and 300°C. Thus, a temperature range of 210 ± 20°C for the diagenesis/anchizone boundary is in agreement with the recent literature. As a consequence, the Steinbruch Schmidt IC values suggest temperatures lower than 210 ± 20°C.

The clay assemblage in the Steinbruch Schmidt section is poorly diversified and dominated only by illite and kaolinite (Fig. 9). A similar poorly diversified association has also been noted by Bauluz Lazaro et al. (1995) for the Devonian of the Iberian Range (Spain) with similar chemical composition for the illitic material which consists of mixtures of illite and ISII interstratified minerals, with a smectite content < 15%. The IC values are typical of the anchizone, and for these authors both illite and kaolinite could be inherited from a highly weathered source area although illite might also have a diagenetic origin. This led to a discussion of the diagenetic or detrital origin of the F/F boundary clays. The diagenetic evolution of the F/F boundary series can lead to chemical transformations of the clays, as the temperature range

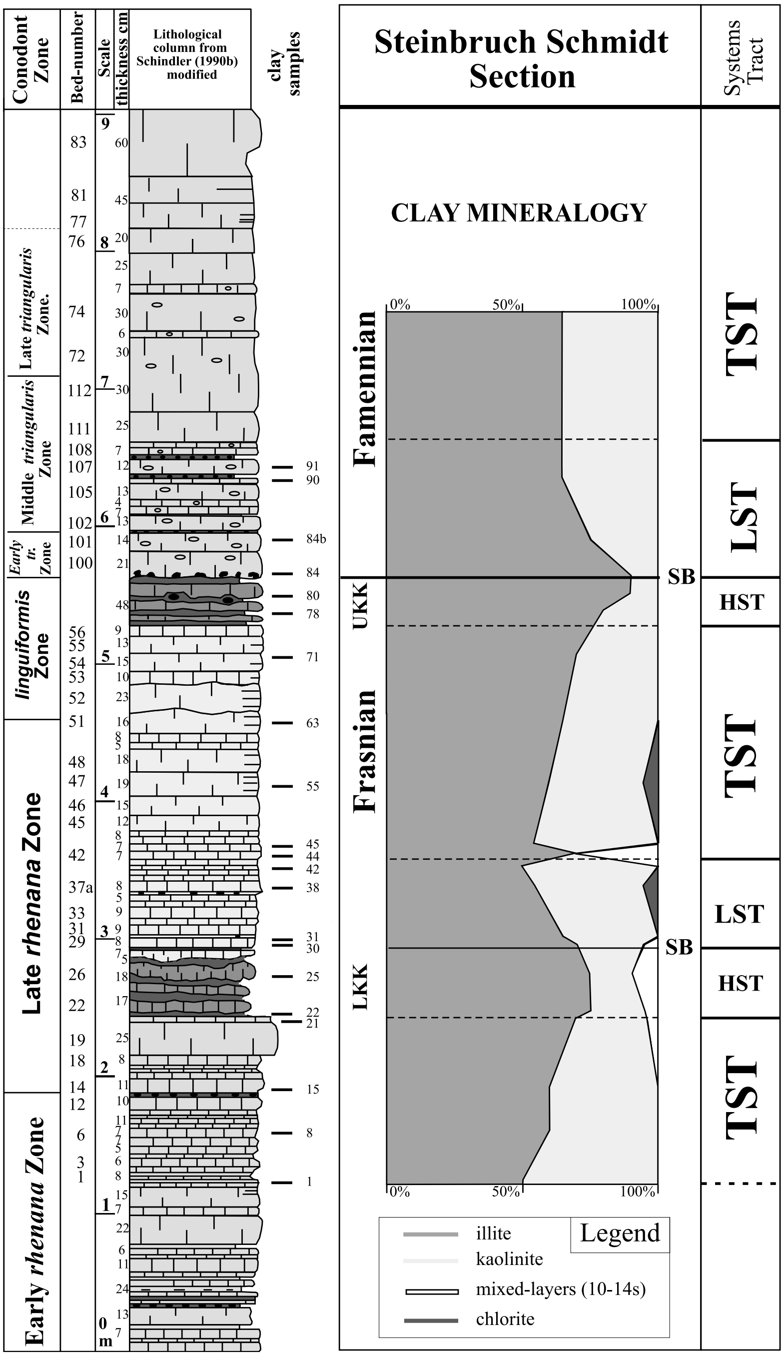

Fig. 9. Lithological column with clay mineralogy results and third-order cycles. A clear increase in illite (and inversely a decrease in kaolinite) is observed in the Kellwasser Horizons. Mixed layers and chlorites are locally present in the Frasnian. Same abbreviations as in Fig. 3.

deduced from the IC is largely sufficient to produce illitisation of smectitic minerals (Chamley, 1989; Han et al., 2000). A part of illite might therefore have a diagenetic origin but a detrital origin cannot be excluded. However, a diagenetic origin for kaolinite is probably not the case since this mineral has been preserved and remains abundant (up to 50%). Moreover, kaolinite has been found in different lithologies (limestones and shales). Thus its relative original percentages have probably been preserved despite the diagenesis. Meanwhile, kaolinite could also appear by authigenesis but this is probably not the case here since this neoformation is essentially reported in highly porous rocks like sandstones and dolostones (Wilson and Pittman, 1977; Chamley, 1989; Lefrancois et al., 1993). The rocks of the studied profile are non-porous shales and fine-grained limestones and unfavourable for kaolinite neoformation. We have also no indication of post-sedimentary fluid effects (no micrite alteration, no dolomitisation, ...) and oxygen isotope values published by McGhee et al. (1986) indicate a range between 4.5 and 5.5‰. These values are very close from those reported by Hurley and Lohmann (1989) for marine FFb signature (4.5 ± 0.5‰) corresponding to the isotope signature of non-luminescent cements of open-marine environments. The oxygen isotope values suggest thus that the FF series of Steinbruch Schmidt experienced no strong diagenetic evolutions linked to post-sedimentary fluid circulation.

A detrital origin for a significant part of the clay mineral assemblages is therefore proposed for the Steinbruch Schmidt section. Fig. 8 gives the clay abundance within the different systems tracts. Kaolinite content decreases from the base of the section up to the LKK, then increases to a maximum between the two Kellwasser Horizons and decreases again to reach a minimum in the UKK. Above the F/F boundary, the kaolinite amount increases to nearly the same percentage as it was at the base of the section. This pattern shows, therefore, that there is no clear difference between the Frasnian and the Famennian clay assemblages with the exception of small quantities of chlorite and mixed layers observed below the UKK. The most striking fact is that kaolinite is at its minimum concentration in the Kellwasser Horizons, thus during the highstand sea levels, and is at its maximum concentration at the end of the regressive episodes (LST). Thus kaolinite increases during the regressive intervals (LST) and decreases during the transgressive ones (TST). The strong increase of kaolinite along the LST is attributed to the gradual development of higher energetic conditions (microbioclastic layers) due to tempestites or turbidites as revealed by the microfacies analysis. This analysis has shown that the microbioclastic layers contain shallow water organisms (algal fragments) and the clay fraction could have been transported from this distant environment and deposited in deeper settings. Thiry and Jacquin (1993) reported a similar case during the Aptian in the Cape basin of South Africa where sandy turbidites are interlayered in carbonaceous black shales. The clay mineral suite of these turbidites is composed of varying amounts of kaolinite, chlorite, illite and traces of mixed layers. Their assemblage, typical of many mudrock successions, is similar to the one of the F/F boundary series, and could support an allochthonous origin (tempestites?) of the kaolinite in the deeper Late Devonian basin. The Kellwasser Horizons deposited during sea-level highstands display the minimum kaolinite content because the environments are the deepest ones and lie below the influence of tempestites.

To summarise, detrital clays supplied from exposed areas have been trapped in a distant shelf and exported basinward after deposition by reworking processes during sea-level falls. Such a situation has already been reported in the Cretaceous palaeoweathering profiles of NW Europe and N America where kaolinite is predominant. The Wealdian terrigenous facies trapped on European shelves and the Cretaceous turbidites filling synrift Atlantic basins are also kaolinite-rich (Thiry and Jacquin, 1993).

Another question must also be solved: why does a high kaolinite percentage (up to 50%) locally occur during Late Devonian times? Robert and Chamley (1991) and Knox (1998) have described such kaolinite enrichment at the Palaeocene/Eocene boundary. In this case, the kaolinite abundance was related to climatic warming: the kaolinite amount increased in the earliest Eocene toward high latitudes indicating intensified humidity on adjacent landmasses where soils were being formed. In the case of the F/F boundary the kaolinite enrichment could also be related to a global warming as suggested by Frakes (1979) and Frakes et al. (1992). Morrow et al. (1996) demonstrated an increase to warmer and drier conditions from Middle Devonian up to Early Carboniferous times. The equatorial Devonian palaeogeographic position proposed by Ziegler (1988) indicates that this warm climate was hot with seasonally restricted rainfall. Kaolinite percentages imply such a hot–wet climate (Chamley, 1989). The Old Red Continent is the only known land area located in a tropical palaeogeographic setting close to the Rhenohercynian basin where the Steinbruch section lies. This land was probably the detrital source for the clays of the Steinbruch Schmidt section. The abundance of kaolinite can probably be attributed to the presence of well-developed kaolinitic soils on the Old Red Continent.

6. Conclusions

(1) Three major microfacies with several lithotypes are present: their succession (MF1–MF3) constitutes the standard sequence of the series and records a shallowing-upward evolution from deep, quiet and poorly oxygenated environments below the storm wave base level to more energetic environments influenced by current activities. The Kellwasser Horizons correspond to the deepest facies (MF1) below the storm wave base. Note that algae, foraminifers, goniatites and radiolarians disappear temporarily at the F/F boundary as well as sponges at each Kellwasser Horizon.

(2) The sequential analysis covering the Lower *rhenana*–Upper *triangularis* conodont Zones shows 11 sub-metric to metric cycles, most of them recording sea-level changes. The cycle stacking and the recognition of two sequence boundaries permits an interpretation of third-order sequences with seven systems tracts. The sequence boundaries are located at the top of the LKK and at the F/F boundary. They are underlined by hardgrounds suggesting time gaps. The Kellwasser Horizons correspond to eustatic highstands. The presence of a layer particularly rich in faunal elements (Schindler, 1993) immediately below the UKK is correlative in our sequential analysis with a TST/HST transition, and could therefore correspond to a maximum flooding surface. This surface is not easily detectable by microfacies analysis in such condensed section.

(3) The comparison of the Steinbruch Schmidt microfacies evolution with the Johnson et al. (1985) curve (T–R cycle IId) shows a similar sea-level evolution. In both cases transgressive evolution during the Kellwasser Horizons and regressive trends above these Horizons are present. Contrary to the Johnson et al. (1985) curve, our detailed microfacies evolution indicates that the transgressions started below the Kellwasser Horizons which correspond therefore only to eustatic highstands.

(4) Late Frasnian sediments (before and during the UKK) show a palmatolepid–polygnathid biofacies suggesting a deposition depth of 100 m or more (Sandberg et al., 1997). All faunas of the Early and Middle *triangularis* Zones contain a mixed palmatolepid (deep)–icriodid (shallow) biofacies indicating a depth from more than 100 m to 60 m (Sandberg et al., 1997). This biofacies change indicates a eustatic fall at the F/F boundary (Sandberg et al., 1988). This sea-level drop is also indicated by the transition from a highstand to a LST. So the conodont biofacies and the evolution of systems tracts follow the same pattern of eustatic changes.

(5) The clay minerals include dominant illite (50–90%) and kaolinite (10–50%), associated with random mixed layers (10–14s) (5–30%) and 5% of chlorite. Quartz and goethite are also present. This assemblage is poorly diversified and similar to the assemblage found in Spain by Bauluz Lazaro et al. (1995) for the same stratigraphic interval.

(6) IC values indicate that the series experienced a high diagenetic grade, but below the diagenesis/anchizone boundary implying a temperature range below 210 ± 20°C.

(7) Kaolinite is abundant (up to 50%) during the LST just above the UKK. The increasing kao-

linite percentage during the LST is related to higher energy conditions (microbioclastic layers) during the sea-level falls. Detrital clays (kaolinite and partly illite) were probably supplied to the deep basin by tempestites or turbidites from a distant shelf located to the north of the Steinbruch Schmidt section.

(8) The high kaolinite percentage suggests a hot–wet climate during the F/F transition. The Old Red Continent seems to be the detrital source of the clays and the kaolinite abundance is related to the presence of well-developed soils on this land area.

Acknowledgements

This paper is part of the PhD work of the first author at the University of Brussels and Lille University. Thanks are due to Professors Mansy and Chamley (Lille University) for easy access to the clay laboratory. G. Racki (Silesian University) is also thanked for FFb fruitful collaboration. This research was undertaken with financial support of the Fonds National de la Recherche Scientifique (Convention 2.4511.94). The paper benefited from many helpful linguistic improvements by M.R. House (University of Southampton) and critical reviews provided by H. Chamley and E. Schindler (Forschungs-Institut Senckenberg) and a third anonymous reviewer. This paper is integrated in the IGCP Programme No. 386.

References

Aigner, T., 1985. Storm depositional systems. In: Coated Lecture Notes in Earth Science 3. Springer, Berlin.

Bauluz Lazaro, B., Burillo, M.J.M., Fernandez-Nieto, C., Lopez, J.M.G., 1995. Mineralogy and geochemistry of Devonian detrital rocks from the Iberian range (Spain). Clay Miner. 30, 381–394.

Baumgartner, P.O., 1987. Age and genesis of Tethyan Jurassic radiolarites. Eclogae Geol. Helv. 80, 831–879.

Baumgartner, P.O., 1990. Genesis of Jurassic Tethyan radiolarites – the example of Monte Nerone (Umbria-Marche Apenninnes). In: Pallini, G. et al. (Eds.), Atti II Conv. Int. F.E.A., Pergola 1987, pp. 19–32.

Beushausen, L., 1900. Das Devon des nördlichen Oberharzes mit besonderer Berücksichtigung der Gegend zwischen Zellerfeld und Goslar. Abh. K. Preuss. Geol. L.-A., N.F. 30, 1–383.

Boulvain, F., 1993. Sédimentologie et diagenèse des monticules micritiques 'F2j' du Frasnien de l'Ardenne. Prof. Pap. no. 260, Ministry of Economic Affairs, Brussels.

Bourque, P.A., Boulvain, F., 1993. Model for the origin and petrogenesis of the red stromatactis limestone of Palaeozoic carbonate mounds. J. Sediment. Petrol. 63, 607–619.

Buggisch, W., 1972. Zur Geologie und Geochemie der Kellwasserkalke und ihrer begleitenden Sedimente (Unteres Oberdevon). Abh. Hess. L.-Amt Bodenforsch. 62, 1–68.

Buggisch, W., 1991. The global Frasnian-Famennian 'Kellwasser Event'. Geol. Rundsch. 80, 49–72.

Casier, J.-G., Lethiers, F., 1998. Ostracods Late Devonian mass extinction: The Schmidt quarry parastratotype (Kellerwald, Germany). C.R. Acad. Sci. Paris 326, 71–78.

Casier, J.-G., Lethiers, F., Baudin, F., 1999. Ostracods, organic matter and anoxic events associated with the Frasnian/Famennian boundary in the Schmidt quarry (Germany). Geobios 32, 869–881.

Chamley, H., 1989. Clay Sedimentology. Springer, Berlin.

Devleeschouwer, X., 1999. The Frasnian/Famennian (Upper Devonian) in Europe: Sedimentology, Sequential Analysis and Magnetic Susceptibility (in French). Unpublished Thesis, University of Brussels, Brussels.

Einsele, G., Ricken, W., Seilacher, A.I. (Eds.), 1991. Cycles and Events in Stratigraphy. Springer, Berlin.

Esquevin, J., 1969. Influence de la composition chimique des illites sur leur cristallinité. Bull. Cent. Rech. Pau S.N.P.A. 3, 147–154.

Feist, R., Schindler, E., 1994. Trilobites during the Frasnian Kellwasser Crisis in European Late Devonian cephalopod limestones. Cour. Forsch.-Inst. Senckenberg 169, 195–223.

Frakes, L.A., 1979. Climates throughout Geologic Time. Elsevier, Amsterdam.

Frakes, L.A., Francis, J.E., Syktus, J.I., 1992. Climate Modes of the Phanerozoic. Cambridge University Press, Cambridge.

Frey, M., 1987. Low Temperature Metamorphism. Blackie, Glasgow.

Friedman, G.M., Sanders, J.E., 1978. Principles of Sedimentology. Wiley, New York.

Garcia-Lopez, S., Brime, C., Bastida, F., Sarmiento, G.N., 1997. Simultaneous use of thermal indicators to analyse the transition from diagenesis to metamorphism: An example from the Variscan Belt of northwest Spain. Geol. Mag. 134, 323–334.

Goodfellow, W.D., Geldsetzer, H.H.J., McLaren, D.J., Orchard, M.J., Klapper, G., 1988. The Frasnian-Famennian extinction: Current results and possible causes. In: McMillan, N.J., Embry, A.F., Glass, D.J. (Eds.), Devonian of the World. Can. Soc. Pet. Geol. Mem. 14, 9–21.

Guernet, C., Lethiers, F., 1989. Ostracodes et recherches des milieux anciens: Possibilités et limites. Bull. Soc. Géol. Fr. 5, 577–588.

Guillocheau, F., Hoffert, M., 1988. Zonation des dépôts de tempêtes en milieu de plate-forme: Le modèle des platesformes nord-gondwanienne et armoricaine à l'Ordovicien et au Dévonien. C.R. Acad. Sci. Paris 307, 1909–1916.

Han, G.M., Préat, A., Chamley, H., Deconinck, J.F., Mansy, J.L., 2000. Palaeozoic clay mineral sedimentation and diagenesis in the Dinant and Avesnes Basins (Belgium, France): Relationships with Variscan tectonism. Sediment. Geol. 136, 217–238.

Holtzapffel, T., 1985. Les minéraux argileux. Préparation. Analyse diffractométrique et détermination. Soc. Géol. Nord 12, 1–136.

Hurley, N.F., Lohmann, K.C., 1989. Diagenesis of Devonian reefal carbonates in the Oscar Range, Canning Basin, Western Australia. J. Sediment. Petrol. 59, 127–146.

Joachimski, M.M., Buggisch, W., 1993. Anoxic events in the Late Frasnian – causes of the Frasnian-Famennian faunal crisis? Geology 21, 675–678.

Joachimski, M.M., Buggisch, W., 1996. The Upper Devonian reef crisis – insights from the carbon isotope record. Gött. Arb. Geol. Paläontol. Sb. 2, 365–370.

Joachimski, M.M., Buggisch, W., Anders, T., 1994. Mikrofazies, Conodontenstratigraphie und Isotopengeochemie des Frasne/Famenne-Grenzprofils Wolayer Gletscher (Karnische Alpen). Abh. Geol. B.-A. 50, 183–195.

Johnson, J.G., Sandberg, C.A., 1988. Devonian eustatic events in the western United States and their biostratigraphic responses. In: McMillan, N.J., Embry, A.F., Glass, D.J. (Eds.), Devonian of the World. Can. Soc. Pet. Geol. Mem. 14, 172–178.

Johnson, J.G., Klapper, G., Sandberg, C.A., 1985. Devonian eustatic fluctuations in Euramerica. Geol. Soc. Am. Bull. 96, 567–587.

Knox, R.W.O'B., 1998. Kaolinite influx within Paleocene/Eocene boundary strata of western Europe. Newsl. Stratigr. 36, 49–53.

Krebs, W., 1979. Devonian basinal facies. Palaeontol. Assoc. Spec. Pap. 23, 125–139.

Kübler, B., 1967. La cristallinité de l'illite et les zones tout à fait supérieures du métamorphisme: Etages tectoniques. Coll. Neuchâtel 1966, 105–121.

Kübler, B., 1968. Evaluation quantitative du métamorphisme par la cristallinité de l'illite: État des progrès réalisés ces dernières années. Bull. Cent. Rech. Pau S.N.P.A. 2, 385–397.

Lefrancois, A., Deconinck, J.-F., Mansy, J.-L., Proust, J.-N., 1993. Structure, sédimentologie et minéralogie des argiles des formations de Beaulieu et d'Hydrequent (Dévonien Supérieur du Bas Boulonnais). Ann. Soc. Géol. Nord 2, 123–134.

Mamet, B., Roux, A., 1975. Algues dévoniennes et carbonifẁres de la Téthys occidentale. 3me partie. Rev. Micropaléontol. 18, 134–187.

Martire, L., 1992. Sequence stratigraphy and condensed pelagic sediments: An example from the Rosso Ammonitico Veronese, northeastern Italy. Palaeogeogr. Palaeoclimatol. Palaeoecol. 94, 169–191.

McGhee, G.R., Jr., Orth, C.J., Quintana, L.R., Gilmore, J.S., Olsen, E.J., 1986. The Late Devonian 'Kellwasser Event' mass extinction horizon in Germany: No geochemical evidence for a large-body impact. Geology 14, 776–779.

Meischner, D., 1971. Clastic sedimentation in the Variscan geosyncline east of the River Rhine. In: Müller, G. (Ed.), Sedimentology of Parts of Central Europe. Int. Sedimentol. Congr., Guidebook 8, Heidelberg, pp. 9–43.

Morrow, J.R., Schindler, E., Walliser, O.H., 1996. Phanerozoic development of selected global environmental features. In: Walliser, O.H. (Ed.), Global Events and Event Stratigraphy in the Phanerozoic. Springer, Berlin, pp. 53–61.

Muchez, P., Boulvain, F., Dreesen, R., Hou, H.F., 1996. Sequence stratigraphy of the Frasnian/Famennian transitional strata: A comparison between South China and southern Belgium. Palaeogeogr. Palaeoclimatol. Palaeoecol. 123, 289–296.

Murphy, A.E., Sageman, B.B., Hollander, D.J., 2000. Eutrophication by decoupling of the marine biogeochemical cycles of C, N, and P: A mechanism for the Late Devonian mass extinction. Geology 28, 427–430.

Préat, A., Mamet, B., Devleeschouwer, X., 1998. Sédimentologie du stratotype de la limite Frasnien-Famennien (Coumiac, Montagne Noire, France). Bull. Soc. Géol. France 3, 331–342.

Reineck, H.E., Singh, I.B., 1975. Depositional Sedimentary Environments. Springer, Berlin.

Robert, C., Chamley, H., 1991. Development of Early Eocene warm climates, as inferred from clay mineral variations in oceanic sediments. Palaeogeogr. Palaeoclimatol. Palaeoecol. 89, 315–331.

Roberts, B., Merriman, R.J., Pratt, W., 1991. The influence of strain, lithology and stratigraphical depth on white mica (illite) crystallinity in mudrocks from the vicinity of the Corris Slate Belt, Wales: Implications for the timing of metamorphism in the Welsh Basin. Geol. Mag. 128, 633–645.

Sandberg, C.A., Morrow, J.R., Warme, J.E., 1997. Late Devonian Alamo impact event, global Kellwasser events, and major eustatic events, Eastern Great Basin, Nevada and Utah. In: Link, P.K., Kowallis, B.J. (Eds.), Proterozoic to Recent Stratigraphy, Tectonics, and Volcanology, Utah, Nevada, Southern Idaho and Central Mexico. Geol. Soc. Am., Field trip Guide Book, Annu. Meet., Salt Lake City, UT, 42, 129–160.

Sandberg, C.A., Ziegler, W., Dreesen, R., Butler, J.L., 1988. Late Frasnian mass extinction: Conodont event stratigraphy, global changes, and possible causes. Cour. Forsch.-Inst. Senckenberg 102, 263–307.

Schindewolf, O.H., 1922. Versuch einer Paläogeographie des europäischen Oberdevons. Z. Dtsch. Geol. Ges. 73, 137–223.

Schindler, E., 1990a. The late Frasnian (Upper Devonian) Kellwasser crisis. In: Kauffman, E.G., Walliser, O.H. (Eds.), Extinction Events in Earth History. Lecture Notes in Earth Sciences 30. Springer, Berlin, pp. 150–159.

Schindler, E., 1990b. Die Kellwasser-Krise (hohe Frasne-Stufe, Ober Devon). Gött. Arb. Geol. Paläontol. 46, 1–115.

Schindler, E., 1993. Event-stratigraphic markers within the Kellwasser Crisis near the Frasnian/Famennian boundary

(Upper Devonian) in Germany. Palaeogeogr. Palaeoclimatol. Palaeoecol. 104, 115–125.

Schlager, W., 1981. The paradox of drowned reefs and carbonate platforms. Geol. Soc. Am. Bull. 92, 197–211.

Schmidt, H., 1928. Exkursion bei Wildungen (Devon, etwas Silur und Karbon). Paläontol. Z. 9, 5–8.

Shirozu, H., Higashi, S., 1972. X-ray examination of sericite minerals associated with the Kuroko deposits. Clay Sci. 4, 137–142.

Środoñ, J., 1984. X-ray powder diffraction identification of illitic materials. Clays Clay Miner. 32, 337–349.

Streel, M., Caputo, M.V., Loboziak, S., Melo, J.-H.G., 2000. Late Frasnian-Famennian climates based on palynomorph analyses and the question of the Late Devonian glaciations. Earth-Sci. Rev. 52, 121–173.

Thiry, M., Jacquin, T., 1993. Clay mineral distribution related to rift activity, sea-level changes and paleoceanography in the Cretaceous of the Atlantic ocean. Clay Miner. 28, 61–84.

Van Wagoner, J.C., Posamentier, H.W., Mitchum, P.M., Vail, P.R., Sarg, J.F., Loutit, T.S., Hardenbol, J., 1988. An overview of the fundamentals of sequence stratigraphy and key definitions. In: Wilgus, C.K., Hastings, B.S., Kendall, C.G.St.C., Posamentier, H.W., Ross, C.H., Van Wagoner, J.C. (Eds.), Sea-level Changes: An Integrated Approach. Soc. Econ. Paleontol. Miner. Spec. Publ. 42, 39–45.

Walliser, O.H., 1980. The geosynclinal development of the Variscides with special regard to the Rhenohercynian Zone. In: Closs, H., Gehlen, K., Illies, H., Kuntz, E., Neumann, J., Seibold, E. (Eds.), Mobile Earth. Int. Geodyn. Proj., Final Rep. FR Germany, pp. 185–195.

Walliser, O.H., 1984. Geologic processes and global events. Terra Cogn. 4, 17–20.

Walliser, O.H., 1988. Proposal for a Frasnian/Famennian Boundary Stratotype. Document submitted to the Devonian Subcommission, I.U.G.S., Rennes.

Walliser, O.H., Lottmann, J., Schindler, E., 1988. Global events in the Devonian of the Kellerwald and Harz Mountains. Cour. Forsch.-Inst. Senckenberg 102, 190–193.

Walliser, O.H., Groos-Uffenorde, H., Schindler, E., Ziegler, W., 1989. On the Upper Kellwasser Horizon (boundary Frasnian/Famennian). Cour. Forsch.-Inst. Senckenberg 110, 247–255.

Warr, L.N., 1996. Standardized clay mineral crystallinity data from the very low-grade metamorphic facies rocks of southern New Zealand. Eur. J. Miner. 8, 115–127.

Warr, L.N., Rice, A.H., 1993. Crystallinity Index Standard. Unpublished Report, Geologisch-Paläontologisches Institut, Heidelberg.

Warr, L.N., Rice, A.H., 1994. Interlaboratory standardization and calibration of clay mineral crystallinity and crystallite size data. J. Metamorph. Geol. 12, 141–152.

Wendt, J., Aigner, T., Neugebauer, J., 1984. Cephalopod limestone deposition on a shallow pelagic ridge: The Tafilalt Platform (Upper Devonian, eastern Anti-Atlas, Morocco). Sedimentology 31, 601–625.

Wilson, M.D., Pittman, E.D., 1977. Authigenic clay in sandstones: Recognition and influence on reservoir properties and paleoenvironmental analysis. J. Sediment. Petrol. 47, 3–31.

Yang, C., Hesse, R., 1991. Clay minerals as indicators of diagenetic and anchimetamorphic grade in an overthrust belt, external domain of southern Canadian Appalachians. Clay Miner. 26, 211–231.

Ziegler, P.A., 1988. Laurussia – the old red continent. In: McMillan, N.J., Embry, A.F., Glass, D.J. (Eds.), Devonian of the World. Can. Soc. Pet. Geol. Mem. 14, 15–48.

Ziegler, W., Sandberg, C.A., 1990. The Late Devonian standard conodont zonation. Cour. Forsch.-Inst. Senckenberg 121, 1–115.